Ferromagnetic Coupling between Semiquinone Type Tridentate Radical Ligands Mediated by Metal Ions

Silvia Bruni,[†] Andrea Caneschi,[‡] Franco Cariati,[†] Chris Delfs,[‡] Andrea Dei,[*,‡] and Dante Gatteschi[‡]

Contribution from the Dipartimento di Chimica, Universita' di Firenze, Firenze, Italy, and Dipartimento di Chimica Inorganica, Metallorganica e Analitica, Universita' di Milano, Milano, Italy

Received August 23, 1993[●]

Abstract: Reactions between 3,5-di-*tert*-butylcatechol, aqueous ammonia and titanium, vanadium, germanium, and tin salts yield neutral bis- complexes of the resulting tridentate Schiff base biquinone ligand. On the basis of their magnetic, electrochemical, and spectral properties all the isolated compounds can be formulated as metal(IV) derivatives of the dinegative radical ligand Cat-N-SQ, M(Cat-N-SQ)$_2$. This suggestion is supported by the structural characterization of the titanium and vanadium derivatives. Both complexes crystallize in the triclinic space group $P1$, with $Z = 2$ in unit cells of the following dimensions: Ti(C$_{28}$H$_{40}$NO$_2$)$_2$ $a = 11.711(4)$ Å, $b = 12.246(5)$ Å, $c = 20.944(10)$ Å, $\alpha = 89.19(4)°$, $\beta = 74.15(4)°$, $\gamma = 75.27(4)°$; V(C$_{28}$H$_{40}$NO$_2$)$_2$ $a = 11.570(3)$, $b = 12.282(8)$, $c = 20.767(13)$ Å; $\alpha = 89.65(5)$, $\beta = 74.58(4)$, $\gamma = 75.98(4)°$. The structural features of the ligands, when compared with those reported earlier for other 3d metal complexes, are in agreement with the proposed charge distribution. This conclusion is also supported by the comparison of the rR spectra of all the 3d metal complexes formed by this Schiff base biquinone ligand. Magnetic and EPR data show that the titanium, germanium, and tin complexes are characterized by triplet ground state arising from the intramolecular ferromagnetic interaction between the two $S = {}^1/_2$ radical ligands. This peculiar magnetic behavior may be rationalized on the basis of the structural properties of these compounds. The role of the metal orbitals in determining the exchange mechanism is discussed. The vanadium complex is characterized by a doublet ground state as a result of the spin coupling between the two radical ligands and the $S = {}^1/_2$ metal ion.

Introduction

Ferromagnetic coupling between organic molecules, although rare, has now been found to be a reality.[1-4] The most spectacular evidence has been found with nitroxide radicals which order as bulk ferromagnets below 2 K,[5] and some very elegant examples of high-spin ground states have been reported for polycarbenes[6-8] and polyarylmethyl polyradicals.[9,10] Spin polarization, according to the model originally suggested by McConnell,[11] is presumably responsible for the spin alignment in the nitroxides, while topological degeneration determines the parallel spin alignment in the polycarbenes.

Beyond these purely organic approaches, attempts have been made to use organic radicals bound to diamagnetic metal ions, which therefore acquire a structural function, properly connecting the organic building blocks in order to give rise to ferromagnetic interactions between them. Furthermore, the metal ions may have an active role in aiding the exchange coupling between the radicals, promoting superexchange interactions between the organic molecules, mediated by their empty and fully occupied orbitals.

Up to now this approach has not yet generated magnetically ordered materials but significant examples of moderate ferromagnetic coupling have been reported. In particular in ferromagnetic chains of imino nitroxides connected by Rh$_2$(carboxylate)$_4$ dimers the coupling was reported to be $J = -5$ cm^{-1} (we use the spin Hamiltonian in the form $\mathcal{H} = J\mathbf{S}_1.\mathbf{S}_2$).[12] The Ga(DTBSQ)$_3$ complex (DTBSQ = 3,5-di-*tert*-butyl-1,2-semiquinonato) was recently found to be characterized by a quartet ground state arising from the ferromagnetic exchange between the three $S = {}^1/_2$ coordinated radical ligands.[13] The observed exchange coupling was $J = -15.6$ cm^{-1}, in agreement with the results of an EPR investigation.[14]

With this in mind we have synthesized titanium(IV), germanium(IV), and tin(IV) complexes of general formula ML$_2$ where L is the dianion of the radical ligand 3,5-di-*tert*-butyl-1,2-semiquinonato 1(2-hydroxy-3,5-di-*tert*-butylphenyl)imine (I, Cat-N-SQ). This ligand, as well the corresponding mononegative quinone (II, Cat-N-BQ), has been shown to be stabilized by coordination to metal ions.[15-17] Structural and magnetic characterization of the 3d metal derivatives from Mn to Zn suggested that they can be formulated as M(Cat-N-SQ)$_2$ (M = Mn(IV)),[16] M(Cat-N-SQ)(Cat-N-BQ) (M = Fe(III), Co(III))[16,17] and M(Cat-N-BQ)$_2$ (M = Ni(II), Cu(II), Zn(II)).[15,17]

[†] Dipartimento di Chimica Inorganica, Metallorganica e Analitica, Universita' di Milano, Italy.

[‡] Dipartimento di Chimica, Universita' di Firenze, Italy.

[●] Abstract published in *Advance ACS Abstracts*, January 15, 1994.

(1) *Magnetic Molecular Materials*; Gatteschi, D., Kahn, O., Miller, J. S., Palacio, F., Eds.; Kluwer Academic Pub.: Dordrecht, 1991.

(2) Buchachenko, A. L. *Russ. Chem. Rev.* **1990**, *59*, 4.

(3) Miller, J. S.; Epstein, A. J.; Reiff, W. M. *Chem. Rev.*,**1988**, *88*, 201.

(4) Miller, J. S., Dougherty, D. A., Eds.; *Mol. Cryst. Liq. Cryst.* **1989**, *176*.

(5) Rassat, A.; Chiarelli, R. In *Magnetic Molecular Materials*; Gatteschi, D., Kahn, O., Miller, J. S., Palacio, F., Eds.; Kluwer Academic Pub.: Dordrecht, 1991; p 191.

(6) Sugawara, T.; Bandow, S.; Kimura, K.; Iwamura, H.; Itoh, K. *J. Am. Chem. Soc.* **1986**, *108*, 368.

(7) Teki, Y.; Takui, T.; Itoh, K.; Iwamura, H.; Kobayashi, K. *J. Am. Chem. Soc.* **1986**, *108*, 2147.

(8) Fujta, I.; Teki, Y.; Takui, T.; Kinoshita, T.; Itoh, K.; Miko, F.; Sawaki, Y.; Iwamura, H.; Izuoka, A.; Sugawara, T. *J. Am. Chem. Soc.* **1990**, *112*, 4074.

(9) Veciana, J.; Rovira, C.; Armet, O.; Domingo, V. M.; Crespo, M. I.; Palacio, F. *J. Am. Chem. Soc.* **1991**, *113*, 2552.

(10) Rajca, A.; Utamapanya, S. *J. Am. Chem. Soc.* **1993**, *115*, 2396.

(11) McConnell, H. M. *Proc. R. A. Welch Found. Chem. Res.* **1967**, *11*, 144.

(12) Cogne, A.; Grand, A.; Rey, P.; Subra, R. *J. Am. Chem. Soc.*, **1989**, *111*, 3230.

(13) Adam, D. M.; Rheingold, A. L.; Dei, A.; Hendrickson, D. N. *Angew. Chem. Int. Ed. Engl.* **1993**, *32*, 391.

(14) Ozarowski, A.; McGarvey, B. R.; El-Hadad, A.; Tian, Z.; Tuck, D. G.; Krovich, D. J.; De Fotis, G. C. *Inorg. Chem.* **1993**, *32*, 841.

(15) Girgis, A. Y.; Balch, A. L. *Inorg. Chem.* **1975**,*14*, 2724.

(16) Larsen, S. K.; Pierpont, C. G. *J. Am. Chem. Soc.* **1988**, *110*, 1827.

(17) Simpson, C. L.; Boone, S. R.; Pierpont, C. G. *Inorg. Chem.* **1989**, *28*, 4379.

0002-7863/94/1516-1388$04.50/0 © 1994 American Chemical Society

The tetrapositive metal ions appear to be particularly well suited in order to stabilize the Cat-N-SQ radical form. Therefore we used the diamagnetic titanium(IV), germanium(IV), and tin(IV) ions, and, for the sake of completeness, vanadium(IV) to bind the radical ligand. We wish to report here the crystal structures of the titanium and the vanadium complexes together with the magnetic properties of all the isolated compounds. Since the ligands are stable in several different oxidation states, every care was used to unequivocally establish their charge. In particular EPR, IR, and electronic spectra were used, together with electrochemical measurements and resonance Raman spectra, which proved to be powerful tools in order to assign the charges to the ligands. For the sake of comparison we investigated also the resonance Raman spectra of the previously reported 3d metal complexes of the Cat-N-BQ and Cat-N-SQ ligands. A preliminary communication of the structure and the magnetic properties of the titanium derivative has been already published.[18]

Experimental Section

Synthetic Procedure. All the complexes were synthesized following the same general procedure. Three milliliters of concentrated aqueous ammonia was added to a solution of 3,5-di-*tert*-butylcatechol (4 mmol) and the appropriate metal salt (1 mmol) in 50 mL of ethanol. Titanium trichloride, vanadium trichloride, germanium tetrachloride, and tin dichloride were used as metal salts. The resulting mixtures were stirred in air at room temperature for 4 h, during which solid crystalline products separated. They were filtered, washed with ethanol, and then recrystallized from dichloromethane–ethanol mixtures. Crystals of the titanium and vanadium derivatives suitable for X-ray analysis were grown by slow evaporation of dichloromethane–ethanol solutions. Anal. Found: titanium C, 75.11; H, 8.95; N, 3.02; vanadium, C, 74.73; H, 8.87; N, 3.15; germanium, C, 72.95; H, 8.84; N, 2.95; tin, C, 69.51; H, 8.24; N, 2.82; $C_{56}H_{80}N_2O_4M$ require: M = Ti, C, 75.30; H, 9.03; N, 3.14; M = V, C, 75.05; H, 9.00; N, 3.13; M = Ge, C, 73.28; H, 8.79; N, 3.05; M = Sn, C, 69.77; H = 8.37; N, 2.91.

The manganese, iron, cobalt, nickel, copper, and zinc derivatives of the diquinone Schiff base ligand were prepared according to literature methods.[15–17]

Physical Methods. Polycrystalline powder EPR spectra were recorded with a Varian E-9 spectrometer working at X-band frequency. Electronic spectra were recorded in the range 5000–40 000 cm^{-1} on a Perkin-Elmer Lambda 9 spectrophotometer. The infrared spectra were recorded on a Perkin-Elmer 283 spectrophotometer. Resonance Raman spectra were measured in dichloromethane solutions (ca. 10^{-2} M) of the samples with a back scattering geometry by a multichannel JASCO TRS-300 spectrophotometer using the lines at 457.9 (21 839 cm^{-1}), 488 (20 492 cm^{-1}) and 514.5 (19 436 cm^{-1}) nm of an argon ion laser and the lines at 568.2 (17 599 cm^{-1}) and at 647.1 (15 433 cm^{-1}) nm of a krypton ion laser. In order to avoid photodecomposition of the samples a rotating cell and a low incident laser power (ca. 50 mW) were used. The magnetic susceptibilities of the compounds were measured in the temperature range 4–300 K in a field of 1 T by using a Metronique Ingenierie MS03 SQUID Magnetometer. Diamagnetic corrections were estimated by Pascal constants. The electrochemical analysis by cyclic voltammetry was carried out using an electrochemical unit (Amel Model 553 potentiostat equipped with Amel 863, 560/A, and 568 elements and an Amel 731 integrator) and a classical three-electrode cell. The working electrode was a platinum microsphere, the auxiliary electrode was a platinum disk, and the reference electrode was a calomel electrode in aqueous saturated KCl (SCE). Before each experiment the solution was carefully deaerated with a nitrogen flow. All potentials here reported are referenced against ferrocenium/ferrocene couple (Fc$^+$/Fc).

Crystallographic Structure Determinations of $Ti(C_{28}H_{40}NO_2)_2$ and $V(C_{28}H_{40}NO_2)_2$. X-ray data were collected on an Enraf Nonious CAD4 four circles diffractometer with Mo K radiation at room temperature. The crystal data for the titanium derivative have been previously reported,[18] and atomic coordinates, bond lengths and angles, and thermal parameters have been deposited at the Cambridge Crystallographic Data Centre. For the vanadium complex the cell parameters were obtained by a least-squares refinement of the setting angles of 19 reflections in the range 9° $\leq \theta \leq$ 15°. Experimental parameters are reported in Table S1 and in a condensed form in Table 2. Data were corrected for Lorentz and polarization effects but not for absorption. The Patterson map revealed the position of the vanadium atom, the positions of the other non-hydrogen atoms were obtained by successive Fourier and difference Fourier syntheses using SHELX88 package. Except hydrogens all the atoms are refined anisotropically. Anisotropic thermal factors are listed in Table S2. The final least-squares refinement converged to $R = 0.073$ and $R_w = 0.080$, respectively. In the structure one *tert*-butyl group was found to exhibit a 2-fold rotational disorder, like the cobalt, manganese, and titanium analogues.[16–18] This group was refined with a variable occupance factor of 49% for not primus atoms. The highest peak in the last difference Fourier map is 0.3 e$^-$ Å^{-3} located in the region of one of the *tert*-butyl. All these groups are affected by thermal motion disorder. Atomic positional parameters are given in Table S2.

Table 1. Crystal Data and Experimental Parameters for $V(Cat\text{-}N\text{-}SQ)_2$

formula	$VC_{56}H_{80}N_2O_4$
crystal system	triclinic
space group	$P1$
a	11.570(3) Å
b	12.282(8) Å
c	20.767(13) Å
α	89.65(5)°
β	74.58(4)°
γ	75.98(4)°
V	2754.7(27) Å^3
Z	2
density (calcd)	1.08 g/cm^3
μ(Mo Kα)	5.66 cm–1
temp	298 K
radiation	Mo K$_\alpha$ (λ = 0.7107 Å)
refinementa[a]	$R = 0.073$
	$R_w = 0.080$

[a] $R = \sum||F_c| - |F_o||/\sum|F_o|$.

Results

Structures. Crystalline compounds of analytical formula ML_2 with M = Ti, V, Ge, and Sn have been obtained, which can in principle be formulated as $M^{II}(Cat\text{-}N\text{-}BQ)_2$, $M^{III}(Cat\text{-}N\text{-}BQ)(Cat\text{-}N\text{-}SQ)$ or $M^{IV}(Cat\text{-}N\text{-}SQ)_2$. In order to elucidate the electronic distribution in these metal complexes, the crystal structures of the titanium and vanadium complexes have been determined.

The molecular structures of the two complexes are quite similar to those reported by Pierpont and co-workers for other 3d metal complexes.[16,17] The ORTEP drawing of the vanadium complex is shown in Figure 1. Selected bond distances and angles are given in Table 2 for the two compounds. The complete data for the vanadium derivative are given in Tables S3–S6. The two complexes are six-coordinate, and the two tridentate ligands occupy the meridional sites of the coordination polyhedron. As observed in the structures of the other 3d metal derivatives, the ligands are not planar. For example, that containing O_1, N_1, and O_2 deviates from planarity, the dihedral angle between the planes of the phenyl rings being 9.7° and 10.0° for the titanium and vanadium, respectively. The other ligand containing O_3, N_2, and O_4 is closer to the planarity, the dihedral angles being 5.4° (titanium) and 5.3° (vanadium). These differences can be attributed to crystal packing effects. The planes of the two ligands in the coordination polyhedron are orthogonal to each other.

A comparison with the structural parameters reported for the nickel(II), cobalt(III), iron(III), and manganese(IV) is shown in Table 3. The observed pattern of the C–O, C–N, and C–C ligand distances in the titanium and vanadium complexes are consistent with the Cat-N-SQ nature of the coordinated ligand, in both the titanium and vanadium derivative. As already discussed by Pierpont and co-workers,[16,17] a well defined correlation exists between the bond distances within the ligand and the electronic structure of the ligand itself. On passing from the mononegative ligand Cat-N-Q to the dinegative Cat-N-SQ, an increase of the C–O and C–N distances is observed. This is accompanied by a

---

[18] Caneschi, A.; Dei, A.; Gatteschi, D. *J. Chem. Soc., Chem. Commun.* **1992**, 631.

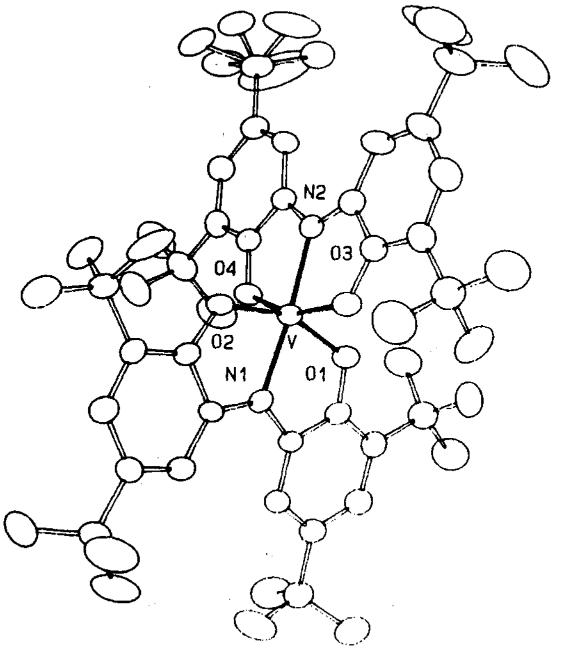

Figure 1. ORTEP view of the asymmetric unit of the V(Cat-N-SQ)$_2$ complex molecule. H atoms are omitted for clarity.

decrease of the C–C$_1$ and C–C$_2$ and by an increase of the C–C$_3$ and C–C$_5$ distances.

These considerations are confirmed by the observed M–O distances, which are within error identical for the titanium, vanadium, and manganese derivatives, suggesting that the two complexes can be formulated as metal(IV) derivatives of the dinegative semiquinonato ligand Cat-N-SQ. The most relevant distinguishing feature in these structures is the M–N distance. This parameter is quite sensitive to the nature of the metal ion being 2.150(6) Å in the titanium, 2.018(5) Å in the vanadium, and 1.910(7) Å in the manganese derivative. The observed trend reflects the expected increasing affinity toward more polarizable donors on passing from titanium to manganese, according to the decreasing hard character of the metal ion. The main consequence of the increasing interaction between the acceptor and the nitrogen donor is reflected in the values of the O$_1$–M–O$_2$ angle which average 151°, 157°, and 165° in the titanium, vanadium, and manganese complexes, respectively. In the cobalt complex, where the M–N distance is even shorter (1.868(5) Å), the O$_1$–M–O$_2$ angle becomes 171°.

Magnetic and EPR Data. All the isolated complexes are paramagnetic. The titanium, germanium, and tin complexes show very similar magnetic behaviors (Figure 2). The titanium complex[18] is characterized by a room temperature $\mu_{\text{eff}} = 2.47\ \mu_B$, slightly higher than expected for two uncorrelated $S = {}^1/_2$ centers within the molecule. On cooling χT increases reaching a plateau in the range 35–4 K corresponding to $\mu_{\text{eff}} = 2.77\ \mu_B$, which is consistent with an $S = 1$ ground state, thus indicating a ferromagnetic interaction between the radical ligands. The fitting of susceptibilty data to a Bleaney–Bowers equation[19] requires $J = -56(1)$ cm^{-1} and $g = 2.00$.

The germanium and tin derivatives are characterized by effective magnetic moments of 2.50 and 2.48 μ_B at room temperature, respectively, and, like titanium, reach values of 2.78–2.79 μ_B at low temperatures. Again it can be concluded that both these complexes are characterized by triplet ground states, as a consequence of the ferromagnetic coupling between the paramagnetic radical centers. The fitting of magnetic susceptibility data yield exchange coupling constant values of –27(1) and –23(1) cm^{-1} for the germanium and tin complexes, respectively, and $g = 2.00$.

Table 2. Selected Bond Distances (Å) and Angles (deg) for V(Cat-N-SQ)$_2$ and Ti(Cat-N-SQ)$_2$[a]

V–O1	1.890(3)	V–O2	1.893(3)
V–O3	1.884(3)	V–O4	1.873(4)
V–N1	2.020(4)	V–N2	2.024(4)
O1–C1	1.323(6)	O2–C15	1.328(6)
O3–C29	1.320(6)	O4–C43	1.332(7)
N1–C6	1.384(5)	N1–C20	1.373(6)
N2–C34	1.379(6)	N2–C48	1.380(7)
C1–C2	1.422(6)	C1–C6	1.406(7)
C2–C3	1.393(8)	C3–C4	1.388(8)
C4–C5	1.382(6)	C5–C6	1.410(7)
C15–C16	1.399(6)	C15–C20	1.423(6)
C16–C17	1.377(8)	C17–C18	1.433(7)
C18–C19	1.340(6)	C19–C20	1.413(7)
C29–C30	1.396(7)	C29–C34	1.414(8)
C30–C31	1.391(8)	C31–C32	1.420(10)
C32–C33	1.360(9)	C33–C34	1.419(7)
C43–C44	1.404(9)	C43–C48	1.424(7)
C44–C45	1.390(9)	C45–C46	1.393(8)
C46–C47	1.369(10)	C47–C48	1.393(8)
Ti–O1	1.898(4)	Ti–O2	1.898(4)
Ti–O3	1.871(5)	Ti–O4	1.878(6)
Ti–N1	2.141(6)	Ti–N2	2.158(6)
O1–C1	1.399(8)	O2–C15	1.333(9)
O3–C29	1.348(8)	O4–C43	1.324(11)
N1–C6	1.370(8)	N1–C20	1.350(9)
N2–C34	1.357(9)	N2–C48	1.374(12)
C1–C2	1.405(9)	C1–C6	1.412(10)
C2–C3	1.409(11)	C3–C4	1.401(11)
C4–C5	1.372(9)	C5–C6	1.416(10)
C15–C16	1.373(9)	C15–C20	1.452(9)
C15–C17	1.383(11)	C17–C18	1.428(10)
C18–C19	1.361(9)	C19–C20	1.409(11)
C29–C30	1.385(12)	C29–C34	1.410(13)
C30–C31	1.401(12)	C31–C32	1.405(15)
C32–C33	1.349(13)	C33–C34	1.431(11)
C43–C44	1.367(15)	C43–C48	1.456(11)
C44–C45	1.437(16)	C45–C46	1.461(14)
C46–C47	1.349(20)	C47–C48	1.402(15)
N1–V–N2	175.2(3)	O4–V–N2	78.5(2)
O4–V–N1	99.5(2)	O3–V–N2	78.1(2)
O3–V–N1	104.0(2)	O3–V–O4	156.4(2)
O2–V–N2	97.5(2)	O2–V–N1	78.1(2)
O2–V–O4	92.7(2)	O2–V–O3	93.5(2)
O1–V–N2	106.0(2)	O1–V–N1	78.4(2)
O1–V–O4	90.6(2)	O1–V–O3	90.7(2)
O1–V–O2	156.4(2)		
N1–Ti–N2	174.5(3)	O4–Ti–N2	76.4(3)
O4–Ti–N1	103.4(3)	O3–Ti–N2	74.6(3)
O3–Ti–N1	105.9(3)	O3–Ti–O4	150.6(3)
O2–Ti–N2	99.4(3)	O2–Ti–N1	75.2(2)
O2–Ti–O4	93.8(3)	O2–Ti–O3	95.2(3)
O1–Ti–N2	109.6(3)	O2–Ti–N1	75.9(2)
O1–Ti–O4	93.4(3)	O1–Ti–O3	92.2(3)
O1–Ti–O2	151.1(3)		

[a] Standard deviations in the last significant digits are given in parentheses.

The above suggestions are supported by EPR data. The spectrum of the frozen solution of the titanium complex in dichloromethane/toluene 1:1 at 4 K (Figure 3) shows the typical features of a triplet spectrum. The feature at $g = 2$ must be attributed to isolated radicals, presumably originated by partial decomposition of the complexes. The standard analysis of the EPR spectra, using the Wassermann equations,[20] yielded $g = 2.0$, $D = 0.014$ cm^{-1}, $E \cong 0$.

The spectra of the germanium(IV) and tin(IV) derivatives are similar, with $g = 2$, and $D = 0.0352$ cm^{-1}, $E \cong 0$ and $D = 0.0635$ cm^{-1}, $E \cong 0$, respectively.

The spectra of the solid compounds show only one quasi-isotropic feature centered at $g = 2$, with a peak-to-peak width of ca. 9 G for titanium, 30 G for germanium, and 200 G for tin. Since triplet spectra are observed for these compounds in solution it can be concluded that intermolecular exchange in the solid averages the fine structure.

Table 3. Metal and Ligand Bond Lengths for Metal–Bis(biquinone) Complexes

	Ti(Cat-N-SQ)$_2$	V(Cat-N-SQ$_2$	Mn(Cat-N-SQ)$_2$[a]	Fe(Cat-N-Q) (Cat-N-SQ)[b]	Co(Cat-N-Q) (Cat-N-SQ)[a]	Ni(Cat-N-Q)$_2$[b]
M–O	1.887(5)	1.888(4)	1.896(5)	1.987(2)	1.896(5)	2.031(2)
M–N	2.150(6)	2.018(5)	1.910*5)	2.117(2)	1.868(5)	2.019(3)
C–O	1.337(9)	1.324(7)	1.325(7)	1.287(3)	1.305(7)	1.264(5)
C–N	1.363(9)	1.380(6)	1.380(7)	1.357(3)	1.361(6)	1.344(5)
C–Cl[c]	1.436(11)	1.424(8)	1.417(8)	1.452(3)	1.445(7)	1.464(4)
C–C2	1.383(13)	1.395(8)	1.408(8)	1.430(3)	1.450(7)	1.450(4)
C–C3	1.409(13)	1.390(9)	1.380(9)	1.368(4)	1.376(7)	1.353(4)
C–C4	1.425(13)	1.411(9)	1.412(8)	1.420(4)	1.426(7)	1.429(4)
C–C5	1.359(12)	1.363(9)	1.367(8)	1.355(3)	1.360(7)	1.344(4)
C–C6	1.415(12)	1.404(8)	1.410(9)	1.420(3)	1.419(7)	1.430(4)

[a] From ref 16. [b] From ref 17. [c] Ligand bond notation from ref 17.

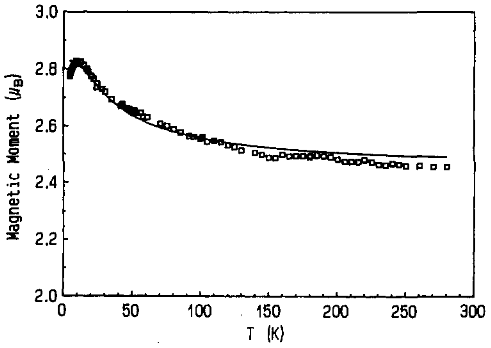

Figure 2. Temperature dependence of magnetic moment for Ge(Cat-N-SQ)$_2$. The solid line represents the calculated values with the best fit parameters (see text).

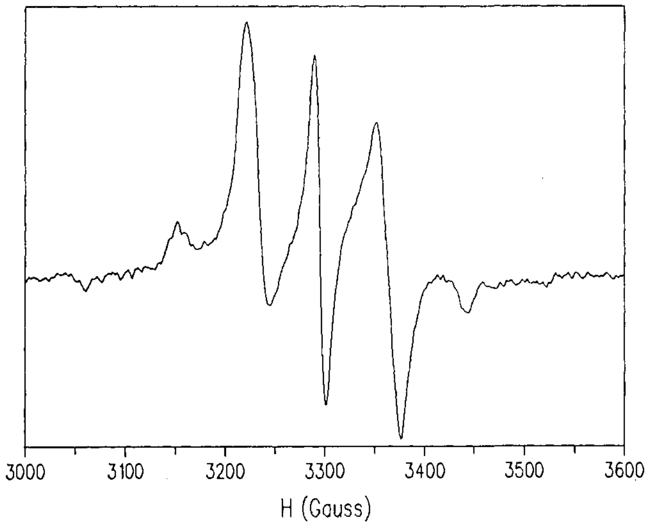

Figure 3. EPR spectrum at 4 K of Ti(Cat-N-SQ)$_2$ in dichloromethane/toluene 1:1.

The vanadium derivative is characterized by a room temperature effective magnetic moment $\mu_{eff} = 1.71\ \mu_B$ and does not show any significant temperature dependence. The observed value is consistent with an $S = {}^1/_2$ ground state of the molecule. The EPR spectra at 4.2 K show a signal centered at $g = 1.99$, both in the solid state and in frozen solution. No hyperfine splitting is observed.

Electronic Spectra. The spectral data of 1,2-dichloroethane solutions of the tin, titanium, and vanadium complexes are reported in Table 4 and Figure 4. The electronic spectra of the tin and germanium chromophores are in practice identical, and for this reason the bands appearing in the spectral range investigated can be attributed to internal transitions of the coordinated Cat-N-SQ ligand. The spectrum of the titanium complex is similar to the above spectra in the low-frequency region below 22 000 cm^{-1}. The additional band at 23 900 cm^{-1} can be tentatively assigned to a ligand-to-metal charge-transfer transition.

The electronic spectrum of the vanadium complex (Figure 4) is quite different from the above spectra and does not contain the pattern of bands characterizing the Cat-N-SQ ligand. In particular it does not contain the strong band at 9800–9900 cm^{-1} which characterizes all the complexes so far isolated containing the radical ligand.[15–17]

Infrared and Resonance Raman Spectra. The infrared spectra of the germanium, tin, and titanium derivatives are similar to each other and to the spectrum of the manganese derivative.[16] In particular they are all characterized by two strong absorptions of similar intensity in the ranges 1305–1315 and 1230–1240 cm^{-1} to be assigned to C–O stretching vibrational modes.

Complexes containing the Cat-N-Q ligand, i.e., the zinc, nickel, and copper derivatives, exhibit a strong absorption in the range 1505–1520 cm^{-1} which we associate with the C=O stretching of the quinone ligand and a strong absorption at 1290 cm^{-1}, also assigned to the C–O stretching mode. The spectrum of the cobalt complex can be considered as due to the sum of the vibrational spectra of species containing the Cat-N-Q and Cat-N-SQ in agreement with the suggested mixed valence character of the coordinated ligands.

The IR spectrum of the vanadium complex leaves some doubt about the charge distribution. In fact two bands are observed at 1313 and 1243 cm^{-1} similar to the titanium, germanium, and tin complexes; however, compared to the latter compounds, these peaks are characterized by a different ratio of intensities, the 1313 cm^{-1} band being significantly weaker than the other.

Resonance Raman spectra of all the 3d metal complexes reported so far with the diquinone ligand were recorded. Using the exciting line at 488 nm we find that copper(II), nickel(II), and zinc(II) derivatives, which contain Cat-N-Q as coordinated ligand, are characterized by identical rR spectra. The spectrum of the copper(II) complex is shown as an example in Figure 5. The band at 1620 cm^{-1} is assigned to the C=N stretching mode, whereas the strong band at 1541 cm^{-1} is assigned to the C=O stretching mode. Following the literature[21] the band around 1380 cm^{-1} can be assigned to a ring vibration characterizing polysubstituted aromatic rings. Finally the band at 1296 cm^{-1} can be assigned to the C–O stretching mode.

Using the same exciting line it was found that the germanium, tin, titanium, and manganese derivatives, which contain the dianionic Cat-N-SQ ligand, show also rR spectra similar to each other, but different from those of the copper(II) derivative. The spectrum of the titanium complex is shown as an example in Figure 6. Compared to Cat-N-Q complexes the C=O stretching band disappears, as expected, while a strong band is observed at 1317 cm^{-1}, which can be assigned to the symmetric stretching of the two C–O bonds. As compared with the latter complexes, it should be pointed out that the C=N band shifts to lower energy falling in the range 1580–1590 cm^{-1}, in agreement with the decreased double bond character. As we have already pointed out, the X-ray structures show that the most prominent difference in these derivatives is the value of the metal–nitrogen distance. Apparently, this difference has no consequences in the IR and rR spectra. The spectrum of the vanadium complex is similar

Table 4. Electronic Spectral Data for $M(Cat\text{-}N\text{-}SQ)_2$ (M = Ti, Ge, Sn, V) in 1,2-Dichloroethane Solutions[a]

metal	spectral data
Ti	9800 (9020), 14 200 (2900), 17 300 (5630), 18 600sh, 23 900 (7765), 28 200 (29 705), 30 400 (30 015), 35 900 (27 335)
Ge	9900 (15 350), 14 800 (2910), 17 900 (6100), 19 200sh, 26 000 (54 380), 27 400 (28 670), 30 900sh, 35 100 (15 350)
Sn	9900 (14 600), 14 600 (2370), 17 500 (5780), 18 900sh, 26 050 (40 960), 27 500 (27 150), 39 900sh, 35 900sh, 35 200 (12 450), 37 200 (14 260)
V	7300 (1465) 11 600sh, 14 000sh, 15 800sh, 18 000 (13 510), 21 000sh, 25 900sh, 27 800sh, 32 700 (20 000), 34 400sh, 38 000sh

[a] Absorption maxima in cm^{-1}; ϵ ($mmol^{-1}$ cm^2) in parentheses; sh = shoulder.

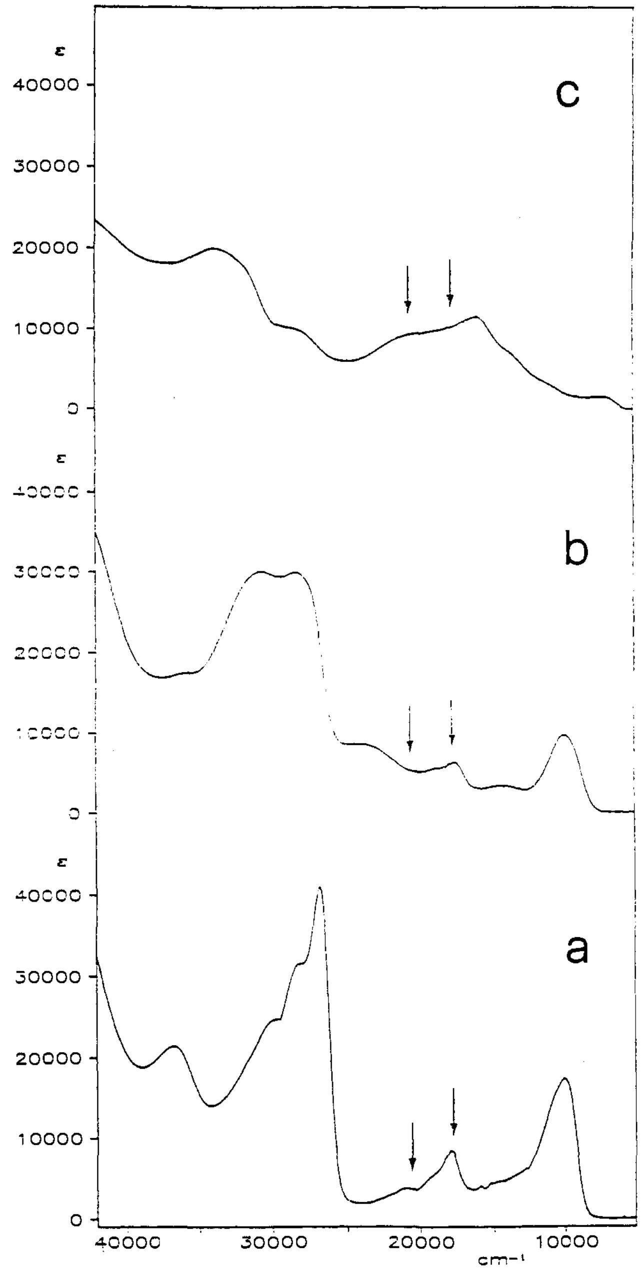

Figure 4. Electronic spectra of (a) $Sn(Cat\text{-}N\text{-}SQ)_2$, (b) $Ti(Cat\text{-}N\text{-}SQ)_2$, and (c) $V(Cat\text{-}N\text{-}SQ)_2$ in 1,2-dichloroethane solution. The arrows indicate the laser frequencies used to excite the rR spectra.

to those of the other $M(Cat\text{-}N\text{-}SQ)_2$ complexes (Figure 7) but is characterized by a lower intensity of the bands. No change in the ligand vibrations is observed for all the $M(Cat\text{-}N\text{-}SQ)_2$ complexes (M = Ti, V, Ge, Sn) using the line at 568.2 nm as the exciting source.

The rR spectra of the iron and cobalt complexes, which contain both the Cat-N-Q and Cat-N-SQ ligands, give different rR spectra depending on the exciting frequency. The electronic spectrum of the Co(Cat-N-BQ)(Cat-N-SQ)[16] can be easily derived as the combination of the spectra of $Sn(Cat\text{-}N\text{-}SQ)_2$ and $Zn(Cat\text{-}N\text{-}BQ)_2$, thus indicating that the optical properties of this chromophore are determined by the internal transitions of the two different ligands. Using the 458-nm exciting line, we found the typical pattern of vibrations characterizing the Cat-N-Q derivatives. On the other hand, using the 514-nm line we found a spectrum which can be considered as containing the vibrations of both electronic forms of the ligands. Similar results were obtained with the iron complex.[15,17] Using the 458-nm line as the source, the rR spectrum of the Cat-N-Q ligand is obtained, whereas using the 647-nm line a spectrum containing the separate vibrations of both the ligands appears. This means that on the rR time scale the ligands are not equivalent, thus indicating that the electron-transfer process between the two ligands occurs at a lower rate than that characterizing the rR technique. This is not an unexpected result since the LUMO of the Cat-N-BQ ligand is orthogonal the SOMO of the Cat-N-SQ, making the electron transfer process unfavourable.

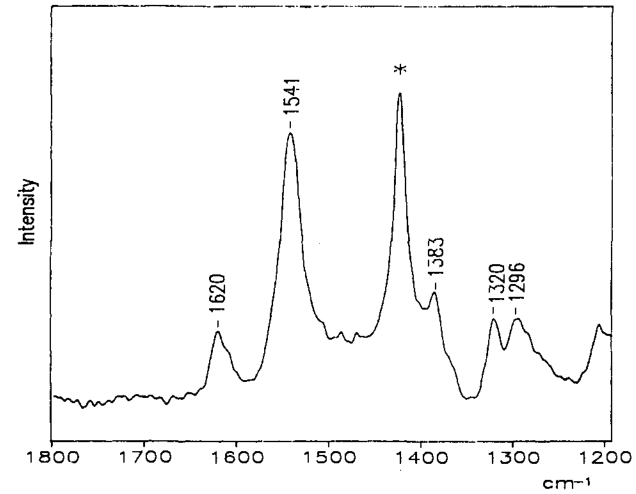

Figure 5. rR spectrum of $Cu(Cat\text{-}N\text{-}BQ)_2$ in dichloromethane solution (excitation at 488 nm); * indicates a solvent band.

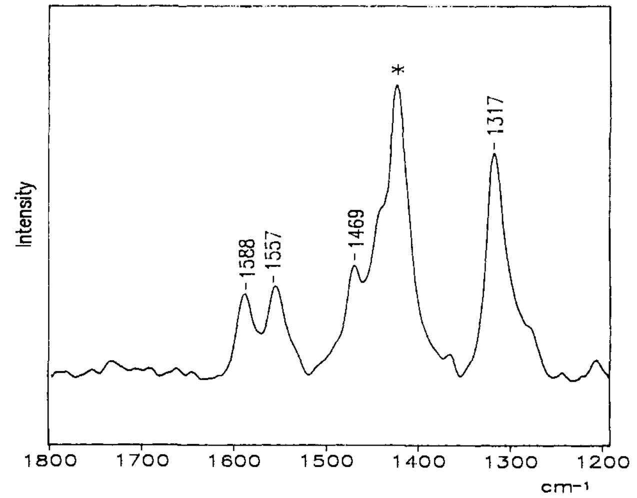

Figure 6. rR spectrum of $Ti(Cat\text{-}N\text{-}SQ)_2$ in dichloromethane solution (excitation at 488 nm); * indicates a solvent band.

Cyclic Voltammetry. Cyclic voltammetry experiments show that the titanium, germanium, and tin derivatives undergo four redox processes in the range −2.0/2.0 V in acetonitrile solution (Table 5). For titanium and tin all the processes appear reversible on the cyclic voltammetry time scale, whereas for germanium the

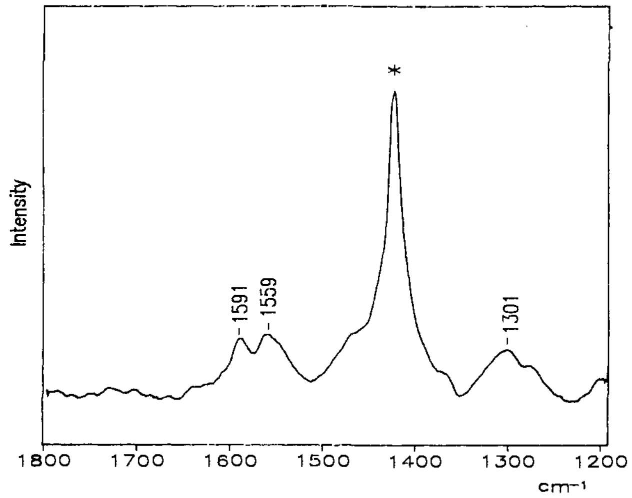

Figure 7. rR spectrum of $V(Cat\text{-}N\text{-}SQ)_2$ in dichloromethane solution (excitation at 488 nm); * indicates a solvent band.

Table 5. Electrochemical Potentials (V) of $M(Cat\text{-}N\text{-}SQ)_2$ Complexes in 1,2-Dichloethane 0.1 M NBu_4PF_6[a,b]

metal	+2/+1	+1/0	0/–1	–1/–2
Ti	0.45	0.08	–0.67	–1.14
Ge	0.55*i*	0.12	–0.70	*i*
Sn	0.57	0.17	–0.67	–1.04
V		0.18	–0.35	–1.78

[a] All potentials are referenced against the ferrocenium/ferrocene couple. The potentials are the average anodic and cathodic peak potentials in cyclic voltammograms recorded at 100 mV s^{-1}; *i* = irreversible process. [b] At 25 °C for ca. 10^{-3} M solutions.

most negative and the most positive ones are not reversible. Coulometric experiments indicate that all the reversible processes are monoelectronic. The three complexes undergo a first oxidation step at a potential in the range 0.08–0.16 V vs Fc^+/Fc followed by a further oxidation step in the potential range 0.46–0.56 V. The two one-electron-transfer processes are necessarily ligand centered and are assigned to the redox couples

$$M(Cat\text{-}N\text{-}Q)(Cat\text{-}N\text{-}SQ)^+ + e^- \rightleftarrows M(Cat\text{-}N\text{-}SQ)_2$$

and

$$M(Cat\text{-}N\text{-}Q)_2{}^{2+} + e^- \rightleftarrows M(Cat\text{-}N\text{-}Q)(Cat\text{-}N\text{-}SQ)^+$$

The two electron-transfer processes occurring at negative potentials are more ambiguous to assign since they may involve either the metal or the ligand. Nevertheless since the first reduction process of the three $M(Cat\text{-}N\text{-}SQ)_2$ derivatives is again characterized by similar potential values, all of them falling in the range –0.66/–0.70 V vs Fc^+/Fc couple, it is reasonable to suggest that this process also involves the coordinated ligand, i.e.,

$$M(Cat\text{-}N\text{-}SQ)_2 + e^- \rightleftarrows M(Cat\text{-}N\text{-}SQ)(Cat\text{-}N\text{-}Cat)^-$$

The second reduction process is impossible to be assigned on the basis of electrochemical data only.

The vanadium derivative undergoes only three one-electron redox processes in the potential range we have considered. The oxidation process occurring at +0.18 V could be associated to an electron-transfer process similar to those occurring in the same potential range we have discussed above, but it should be pointed out that it is not followed by any other redox process. The first reduction process, which occurs at –0.35 vs Fc^+/Fc, could be tentatively suggested to involve the metal ion, but more data are required in order to formulate any conclusion.

Discussion

The results reported here show how the orthogonality of magnetic orbitals can be achieved in complexes containing two organic radicals by using appropriate diamagnetic acceptors and properly designed ligands. Here tetravalent titanium, germanium, and tin ions have been used for stabilizing the dinegative tridentate radicals Cat-N-SQ in a pseudooctahedral polyhedron. According to their structural and electronic properties, the two ligands occupy the meridional sites of the coordination polyhedron. Assuming an overall C_{2v} symmetry for these complexes, the two π^* magnetic orbitals behave as b_1 and b_2, respectively, and are therefore orthogonal to each other, thus justifying the observed ferromagnetic coupling. We suggest that the radical orbitals interact by a super exchange mechanism mediated by the metal orbitals, as previously observed in other compounds in which pairs of organic radicals are connected by a diamagnetic metal ions.[12,23,24] The role of the metal ions is to provide orbitals of appropriate energy and symmetry, i.e., $3d\pi$ for titanium and np for germanium and tin, which provide a mechanism for the exchange coupling interaction.

The exchange mechanism may be due both to direct overlap between the ligand magnetic orbitals and to superexchange mediated by the metal orbitals. The shortest interligand oxygen–oxygen distances in the titanium derivative are ca. 2.7 Å. Although they are relatively long, some interaction through this mechanism cannot be ruled out. In fact sizable coupling has been observed between nitroxides separated by as much as 3.13 Å.[22] However in this way it does not seem easy to justify the large decrease of the coupling constant on passing from titanium to germanium and tin. Assuming an exponential decay of the coupling constant with the distance between the paramagnetic centers, the shortest contacts between the oxygen atoms of L in germanium and tin should be ca. 3.4 Å. This would require major distortions from the structure observed for the titanium complex. Of course minor deformations tending to give some nonzero overlap between the ligands cannot be ruled out for germanium and tin, for which no structural data are available.

On the other hand superexchange mediated by metal orbitals can also be operative. The π^* orbital can overlap with both fully and empty metal obitals. Titanium(IV), which is isoelectronic to chloride ion, has both full $3p$ and empty $3d$ orbitals available. Since the lowest charge-transfer transition is likely ligand to metal in nature, it is conceivable that superexchange is transmitted by the empty d orbitals. The mechanism for germanium(IV) and tin(IV) may involve the empty np orbitals, which are less well matched with the radical orbitals, thus determining a weaker coupling.

Finally, it should be mentioned that a similar mechanism has been found to be operative in the $Ga(DTBSQ)_3$ complex (DTBSQ = 3,5-di-*tert*-butyl-*o*-semiquinonato), which is characterized by a quartet ground state.[13] For this complex symmetry considerations alone would predict a doublet ground state, according to the D_3 symmetry of this compound.

The EPR spectra of the solutions of the titanium, germanium, and tin derivatives show a well-resolved fine structure, which deserves some additional comments. The dipole–dipole interactions should be the dominant contributions to the zero field splitting in the titanium complex, whereas in the complexes with heavier metal ions spin-orbit coupling effects may be of some importance. The broad lines observed for the germanium and tin derivatives did not allow us to check if significant deviations from $g = 2$ are observed, which would confirm large spin orbit admixture of excited states.

The dipole contribution to the D tensor has been calculated using two different methods. In both approaches the crystallographic positions of the atoms were used, and the *tert*-butyl groups were replaced with hydrogens.

The extended Huckel method was used to calculate the molecular orbitals of the radical ligands, and a numerical integration procedure was used to evaluate the integrals necessary for the dipole tensor. The single-ζ radial functions and the H_{ii}

parameters required for the extended Huckel calculations were taken from the literature.[25] The coordinate system used for the calculations was defined such that the x axis was parallel to the Ti-N1 bond and the xy plane was defined by the N1-Ti-O1 bond. The procedure for the numerical integrations is given in ref 26. The resulting dipole tensor was then diagonalized, and the D and E parameters were determined from standard relations.

The dipole tensor was also calculated by a second method which has given good results for other workers in this area in the past.[27] This approach uses the point dipole approximation and assumes that the spin density occupies the p_z atomic orbitals of the radical anions. Each p orbital is approximated by point dipoles placed 0.7 Å above and below the atomic position along the z axis. The dipole tensor is then calculated by summing all of the contributions from each pair of point dipoles. Performing both calculations serves as a check on the validity of the other.

	D	E	E/D
numerical integration	0.0112	0.000172	0.015
point dipole	0.0118	6.2 × 10–5	0.005
experiment	0.014		

The results of the calculations clearly agree well with both each other and reasonably well with the experimentally determined value. The principal D_{zz} axis of the dipole tensor points along the N1-Ti-N2 axis which is as expected for such a system. The two methods give different directions for the x and y axes of the dipole tensor but since the calculated orthorhombic component E is so small this is not considered important.

The vanadium complex deserves a different comment. The structural parameters are consistent with a $\mathrm{V^{IV}(Cat\text{-}N\text{-}SQ)_2}$ formulation, but some spectroscopic data, the ESR and electronic spectra in particular, fail to provide unequivocal support to that hypothesis. In fact the magnetic data which show a ground $S = {}^1/_2$ state require a strong antiferromagnetic exchange mechanism between the $S = {}^1/_2$ metal ion and the coordinated radicals. For exchange coupled symmetrical triads of paramagnetic centers the relationship

$$g = {}^4/_3 g_{\mathrm{semiq}} - {}^1/_3 g\mathrm{V(IV)}$$

should be operative.[28] Since the semiquinonato g value is 2.00 and that of vanadium(IV) is smaller than 2, the g value for the triad should be larger than 2, contrary to the experimental result. The EPR data in conclusion suggest that there is an extensive admixture of the vanadium and ligand orbitals.

Alternate formulations as $\mathrm{V^{III}}$(Cat-N-Q)(Cat-N-SQ) and $\mathrm{V^{V}}$-(Cat-N-Cat)(Cat-N-SQ) may also account the charge neutralization of the system and its doublet ground-state magnetic properties, but again none of these formulations is fully consistent with the spectroscopic results. In practice, as a contrast with the other 3d metal complexes formed by these tridentate Schiff base ligands, it is quite hard to describe this system in terms of a localized structure described by only one electronic isomer, a delocalized structure seems more appropriate. The lack of any absorption associated to C=O stretching mode either in the IR and rR spectra suggests that a tentative description could be the one intermediate between the $\mathrm{V^{V}}$(Cat-N-Cat)(Cat-N-SQ) and $\mathrm{V^{IV}(Cat\text{-}N\text{-}SQ)_2}$. The presence of several low-energy transitions in the electronic spectra might be consistent with this description.

Conclusions. The examples reported here show how large ferromagnetic coupling can be achieved with suitably designed radicals and open a new perspective for the design of molecular based ferromagnets. The large ferromagnetic couplings observed for these complexes indicate that this strategy might undoubtedly offer a valid alternative to those we have mentioned in the introduction for achieving this goal. We are currently attempting to design a bistridentate radical anion, able to bridge two different diamagnetic or paramagnetic metal ions, thus yielding a sequence of ferromagnetically coupled paramagnetic moieties.

Acknowledgment. This work was financially supported by M.U.R.S.T. and C.N.R., progetto finalizzato "Materiali Speciali Per Tecnologie Avanzate".

Supplementary Material Available: Tables of data collection information, atom coordinates, bond lengths and angles, atomic positional parameters and isotropic thermal factors, calculated positional parameters for hydrogen atoms, and anisotropic thermal factors (15 pages). This material is contained in many libraries on microfiche, immediately follows this artile in the microfilm version of the journal, and can be ordered from the ACS; see any current masthead page for ordering information.

---

(19) Bleaney, B.; Bowers, D. K. *Proc. Roy. Soc. London* Ser. A **1952**, *214*, 451.

(20) Wasserman, A.; Snyder, L. C.; Yager, W. A. *J. Chem. Phys.* **1964**, *41*,

(21) Dollish, F. R.; Fateley, W. G.; Bently, F. F. *Characteristic Raman Frequencies of Organic Compounds;* John Wiley: New York, 1974.

(22) Caneschi, A.; Gatteschi, D.; Laugier, J.; Rey, P.; Sessoli, R. *Inorg. Chem.* **1988**, *27*, 1553.

(23) Benelli, C.; Caneschi, A.; Gatteschi, D.; Pardi, L.; Rey, P. *Inorg. Chem.* **1989**, *28*, 3230.

(24) Benelli, C.; Caneschi, A.; Gatteschi, D.; Pardi, L.; Rey, P. *Inorg. Chem.* **1989**, *28*,275.

(25) Tatsumi, K.; Hoffman, R. J. *J. Am. Chem. Soc.* **1981**, *103*, 3328.

(26) Gribnau, M. C. Ph.D. Thesis, University of Nijmegen, The Netherlands, 1988.

(27) Ozarowski, A.; McGarvey, B. R.; Peppe, C.; Tuck, D. G. *J. Am. Chem. Soc.* **1991**, *113*, 3288.

(28) Bencini, A.; Gatteschi, D. *EPR of Exchange Coupled Systems*, Springer-Verlag: Berlin, Heidelberg, 1990.